Climate extremes and predicted warming threaten Mediterranean Holocene firs forests refugia

Raúl Sánchez-Salguero[a,b,1], J. Julio Camarero[a], Marco Carrer[c], Emilia Gutiérrez[d], Arben Q. Alla[e], Laia Andreu-Hayles[f,g], Andrea Hevia[h], Athanasios Koutavas[i], Elisabet Martínez-Sancho[j], Paola Nola[k], Andreas Papadopoulos[l], Edmond Pasho[e], Ervin Toromani[e], José A. Carreira[m], and Juan C. Linares[b]

[a]Instituto Pirenaico de Ecología–Consejo Superior de Investigaciones Científicas, 50192 Zaragoza, Spain; [b]Departamento Sistemas Físicos, Químicos y Naturales, Universidad Pablo de Olavide, 41013 Sevilla, Spain; [c]Dipartimento Territorio e Sistemi Agro-Forestali, Università degli Studi di Padova, Legnaro 35020, Italy; [d]Departamento Biologia Evolutiva, Ecologia i Ciències Ambientals, University of Barcelona, 08028 Barcelona, Spain; [e]Fakulteti i Shkencave Pyjore, Universiteti Bujqësor i Tiranës, 1029 Tirana, Albania; [f]Tree-Ring Laboratory, Lamont-Doherty Earth Observatory, Palisades, NY 10964; [g]Institut Català de Ciències del Clima, 08005 Barcelona, Spain; [h]Forest and Wood Technology Research Centre, 33936 Siero, Asturias, Spain; [i]Department of Engineering Science and Physics, College of Staten Island, City University of New York, Staten Island, NY 10314; [j]Department of Ecology and Ecosystem Management, Technische Universität München, 85354 Freising, Germany; [k]Dipartimento Scienze della Terra e dell'Ambiente, Università degli Studi di Pavia, 27100 Pavia, Italy; [l]Department of Forestry and Natural Environment Management, Technological Educational Institute of Stereas Elladas, 36100 Karpenissi, Greece; and [m]Centro de Estudios Avanzados de la Tierra, Universidad de Jaén, 23071 Jaén, Spain

Edited by William H. Schlesinger, Cary Institute of Ecosystem Studies, Millbrook, NY, and approved September 29, 2017 (received for review May 16, 2017)

Warmer and drier climatic conditions are projected for the 21st century; however, the role played by extreme climatic events on forest vulnerability is still little understood. For example, more severe droughts and heat waves could threaten quaternary relict tree refugia such as Circum-Mediterranean fir forests (CMFF). Using tree-ring data and a process-based model, we characterized the major climate constraints of recent (1950–2010) CMFF growth to project their vulnerability to 21st-century climate. Simulations predict a 30% growth reduction in some fir species with the 2050s business-as-usual emission scenario, whereas growth would increase in moist refugia due to a longer and warmer growing season. Fir populations currently subjected to warm and dry conditions will be the most vulnerable in the late 21st century when climatic conditions will be analogous to the most severe dry/heat spells causing dieback in the late 20th century. Quantification of growth trends based on climate scenarios could allow defining vulnerability thresholds in tree populations. The presented predictions call for conservation strategies to safeguard relict tree populations and anticipate how many refugia could be threatened by 21st-century dry spells.

Abies spp. | climate change | dendroecology | emission scenarios | forward growth model

Climate is a major driver of long-term changes and shifts in tree species distribution (1). Forecasts for the 21st century predict an increase of up to 6 °C in mean temperature, as well as more severe and lasting dry spells and heat waves (2). Climate extremes can play a key role, albeit little explored, in affecting the functioning and vulnerability of drought-prone relict forests (3) and in triggering forest die-off (4) with cascading effects on biodiversity, carbon, water, and nutrient cycling, and ultimately on the provisioning of forest ecosystem services (5).

The persistence of tree species under new climatic conditions will depend upon their ability to acclimatize or buffer climate extremes (6). Special attention needs to be paid to tree-species refugia, i.e., sites where the species persisted during glaciations and currently form relict or isolated stands (7). Relict fir populations located in Circum-Mediterranean fir forests (CMFF), where water availability is the major forest growth constraint, could be threatened by the forecasted warmer and drier conditions (8). In addition, drought stress could also be amplified by forecasted hot temperature extremes (9). Understanding how these populations would respond to the predicted climate warming and amplified drought stress is relevant to forecasting how and where biodiversity refugia would endure adverse climates extremes during the 21st century (10).

Circum-Mediterranean firs (*Abies* species) constitute an example of endangered forests and an ecosystem highly vulnerable to climate warming (11). The intense habitat fragmentation and degradation as a result of anthropogenic activities has reduced their population sizes in the Modern Era and increased the extinction risk for some of these taxa (12–14). More severe droughts could reduce the present ranges of Circum-Mediterranean firs, particularly the dry (southernmost or lowermost) distribution limits, but also in xeric sites (15). This calls for a better assessment of the CMFF vulnerability to projected climate warming and extreme climatic events. Comparing forest growth responses to observed and forecast climate can provide the right avenue to quantify CMFF vulnerability.

The susceptibility of trees to extreme climatic events such as droughts is usually expressed by low radial-growth rates beyond a critical minimum threshold (4). Many investigations confirmed that extensive growth reduction can be considered as an early warning signal of stand vulnerability to episodes of drought- and/or heat-triggered dieback (5, 16–20) with, in the most critical circumstances, cascade effects on local contraction of the species distribution area (21–24). Time series of tree-ring width indices (TRWi) coupled

Significance

Climate extremes are major drivers of long-term forest growth trends, but we still lack appropriate knowledge to anticipate their effects. Here, we apply a conceptual framework to assess the vulnerability of Circum-Mediterranean *Abies* refugia in response to climate warming, droughts, and heat waves. Using a tree-ring network and a process-based model, we assess the future vulnerability of Mediterranean *Abies* forests. Models anticipate abrupt growth reductions for the late 21st century when climatic conditions will be analogous to the most severe dry/heat spells causing forest die-off in the past decades. However, growth would increase in moist refugia. Circum-Mediterranean fir forests currently subjected to warm and dry conditions will be the most vulnerable according to the climate model predictions for the late 21st century.

Author contributions: R.S.-S., J.J.C., and J.C.L. designed research; R.S.-S., J.J.C., M.C., E.G., A.H., and J.C.L. performed research; R.S.-S., J.J.C., A.H., and J.C.L. contributed new reagents/analytic tools; R.S.-S., J.J.C., M.C., E.G., A.Q.A., L.A.-H., A.K., E.M.-S., P.N., A.P., E.P., E.T., J.A.C., and J.C.L. contributed to field data; R.S.-S., J.J.C., A.H., and J.C.L. analyzed data; and R.S.-S., J.J.C., M.C., E.G., A.Q.A., L.A.-H., A.H., A.K., E.M.-S., P.N., A.P., E.P., E.T., J.A.C., and J.C.L. wrote the paper.

The authors declare no conflict of interest.

This article is a PNAS Direct Submission.

Data deposition: The datasets reported in this paper have been deposited in the Pangaea repository, https://doi.org/10.1594/PANGAEA.882101.

[1]To whom correspondence should be addressed. Email: rsanchez@upo.es.

This article contains supporting information online at www.pnas.org/lookup/suppl/doi:10.1073/pnas.1708109114/-/DCSupplemental.

with process-based forward models of growth offer a valuable tool for understanding forest growth responses to climate change (25). We projected the radial growth of CMFF (*SI Appendix*, Fig. S1 and Table S1) as a function of different 21st-century climate forecasts under two contrasting representative emission scenarios (Representative Concentration Pathways, or RCPs) (2, 26), applying the Vaganov–Shashkin–Lite model (hereafter VS-Lite model) (27, 28). We analyzed climate-growth associations paying special attention to the stability of Mediterranean fir refugia under climate extremes (see the conceptual framework in Fig. 1).

Results and Discussion

We detected a generally positive influence on tree growth by previous late-summer wet and cool climatic conditions but a high site-to-site variability in the climate-growth relationships within each species (*SI Appendix*, Fig. S2). Years with significant growth reduction (negative pointer years) usually corresponded to heat waves and dry spells (*SI Appendix*, Figs. S3 and S4). Forecasted warmer and drier conditions corresponding to the RCP 8.5 scenario projected a growth decline at lower latitudes and elevations (Fig. 2 and *SI Appendix*, Fig. S3 and Table S2), although still with a high inter- and intraspecific variability.

Assessment of Extremes Using Process-Based Growth Models. The VS-Lite model accurately tracked the year-to-year growth variability (Fig. 3 and *SI Appendix*, Figs. S6 and S7 and Tables S3 and S4). The growth response to temperature (gT) peaked during the growing season (May to September) in strictly Mediterranean firs (15), while the growth response to moisture (gM) dropped during summer in response to dry conditions (Fig. 3). Tree growth was limited by low temperatures ($gT < gM$) at the beginning and end of the growing season and by soil moisture availability ($gM < gT$) from late spring to autumn.

Changes in the Climatic Thresholds of Circum-Mediterranean Firs. Under the warmest climate scenario (RCP 8.5), several Mediterranean firs (Figs. 4 and 5) are predicted to be increasingly constrained by soil moisture availability, i.e., more drought stress throughout the growing season (Figs. 4 and 5). Some fir species will experience persistent dry conditions at levels similar to those during 20th-century extreme dry spells (Figs. 3–5 and *SI Appendix*, Fig. S8). On the contrary, the wettest sites are predicted to have an extended growing season (*SI Appendix*, Fig. S9).

We provide empirically based constraints on modeled climate-induced changes in growth for CMFF and present an approach

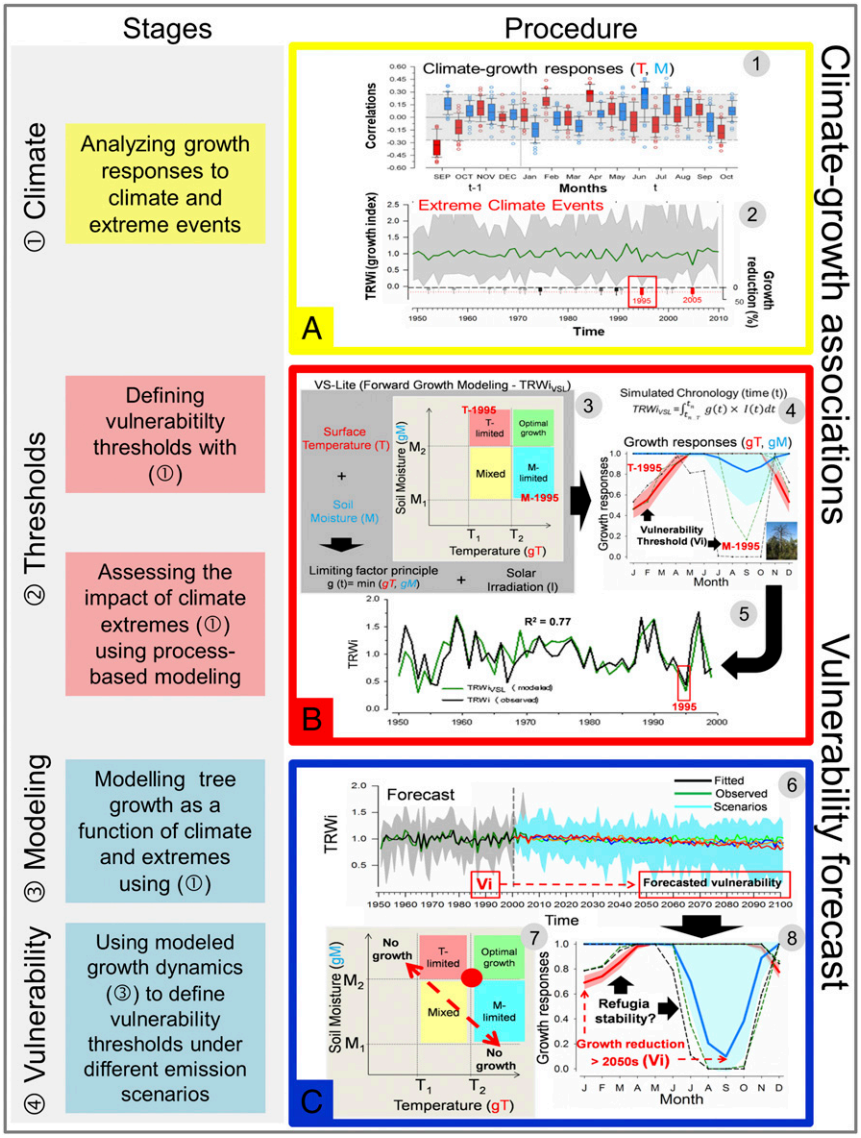

Fig. 1. Conceptual framework for assessing forest vulnerability to climate change based on growth responses to extreme climate events. The figure shows the framework stages (*Left* column) and the procedures and tools used to fulfill this approach (*Right* column). (*A*) We quantified, for each site, how growth responds to climatic conditions and extreme climatic events using correlation coefficients between the mean series of TRWi and mean temperature (red) or total precipitation (blue) (1). Temporal window spans depend on the species and location [e.g., from previous ($t-1$) September up to current (t) October]. Significant ($P < 0.05$) values are located outside the dashed lines. We analyzed the impact of critical climate variables on growth using extreme pointer year analyses (2). Extreme negative growth years (very low TRWi values) corresponding to >50% raw growth reduction in more than 50% of trees on a site were selected (red squares). (*B*) To define the vulnerability threshold, we simulated TRWi using the VS-Lite process-based growth model (3) in which several parameters are estimated: temperature (T_1) or soil moisture (M_1) thresholds below which growth will not occur, optimal temperature (T_2), or soil moisture (M_2) above which growth is not limited (*Materials and Methods*; *B*, 3 is adapted from ref. 76). Growth depends on temperature (gT, red lines and red areas correspond to the mean and SD, respectively) and soil moisture limitations (gM, blue lines and blue areas correspond to the mean and SD, respectively). Note that high-gT or low-gM values indicate low and high growth limitations, respectively. Observed years with extremely low growth (e.g., 1995) based on observed drought- or heat-induced dieback episodes are indicated as vulnerability threshold (Vi) (critical tipping thresholds of growth stability are indicated by black dashed lines) (4). To model growth responses as a function of climate extremes and to define vulnerability thresholds, we compared observed and simulated (VS-Lite) TRWi series (5). (*C*) We compared observed and projected TRWi based on stepwise multiple linear regressions using emission and climate scenarios as predictors (6). Simulated (VS-Lite) growth responses were compared with extreme years under future climate scenarios (2050–2100) (7). The observed gT and gM values defined the observed vulnerability thresholds for each forest refugia comparing projected growth responses with forecasted climate scenarios (8).

that accounts for intraspecific traits and geographic shifts in climate response to forecasted 21st-century extreme events (Fig. 1). This represents an important advance in quantifying ecological responses to future climatic constraints since conservation of marginal tree populations will depend not only on climate forcing, but also on adequately considering vulnerability thresholds (29–31). Our projections question the role of long-term evolutionary buffering effects on some relict Circum-Mediterranean fir species and highlight the impacts of forecasted 21st-century climate variability on the stability of climatic tree refugia (32) (Fig. 5).

We projected stable growth conditions for some species (e.g., *A. alba* and *A. borisii-regis*) in the northern Mediterranean Basin under the moderate RCP 4.5 warming scenario, but a substantial decline in southern populations under the significantly warmer RCP 8.5 (Figs. 4 and 5 and *SI Appendix*, Fig. S8). On the contrary, growth enhancement due to a longer growing season is predicted at high-elevation (wettest) sites (33, 34) (Fig. 2 and *SI Appendix*, Table S2). We also expect that some species (e.g., *A. cephalonica*, *A. pinsapo*, and *A. cilicica*) growing in dry and low-elevation sites may be strongly and negatively influenced by warming-induced drought stress and will be the most sensitive to climate extremes under the RCP 8.5 scenario (Fig. 3 and *SI Appendix*, Fig. S3).

This implies that some forest stands will be unlikely to keep pace with the enhanced decline forecast for the late 21st century, especially given that several episodes of long-lasting reductions in growth, linked to subsequent tree mortality (17, 20, 35), have already been observed in different dry regions of southern and central Europe (19, 20, 36). Our findings support the predictions of range contractions, local extinctions, and species composition changes in many fir stands due to warming temperatures (23) and the increasing frequency of drought-triggered dieback (5, 21, 22, 24, 37). Within this scenario, the increase in water-use efficiency related to rising atmospheric CO_2 concentrations could ameliorate drought resistance in some species (38) but not necessarily with a corresponding effect on growth (39, 40).

Following a drought avoidance strategy (15), *A. cephalonica* copes better with long-term droughts than *A. borisii-regis* and can thus be found on a greater variety of substrates, including dry compact limestones. In contrast, *A. borisii-regis* occurs in more humid sites and at higher latitudes (41) (*SI Appendix*, Table S5). Our analyses suggest that for *A. borisii-regis* higher spring temperatures will negatively affect tree growth characteristics (Fig. 5). Something similar is currently observed in *A. alba*, where increased solar radiation accompanied by low rainfall and warmer temperatures had a negative effect on growth as less sunshine seemed to be sufficient for an adequate photosynthetic carbon assimilation in this shade-tolerant species (42).

In the case of *A. cilicica* and *A. pinsapo* under a hypothetical moderate temperature increase (RCP 4.5 scenario) and if rainfall remained stable, the species' growth responses would not be greatly disrupted (*SI Appendix*, Figs. S5 and S8). In contrast, a temperature increase in the previous autumn and winter may make these species more sensitive to cold spells in winter (15) (*SI Appendix*, Table S6). Warm autumns may also lead to a depletion of reserves as a result of the prevalence of respiration over photosynthesis having a negative impact on growth in the next year (43).

Mediterranean firs show adaptive features to increasing drought stress by adjusting their phenology and hydraulic architecture (e.g., leaf area to sapwood area ratio) to local climatic conditions, particularly the most widespread species (44). The wide intersite variability in modeled VS-Lite parameters (Fig. 5 and *SI Appendix*, Table S4) may arise from parallel intersite differences in environmental conditions or from contrasting interspecies drought tolerance caused by local genetic adaptation and phenotypic plasticity (45). Anatomical and physiological studies suggest that, for some of these species, there is an early

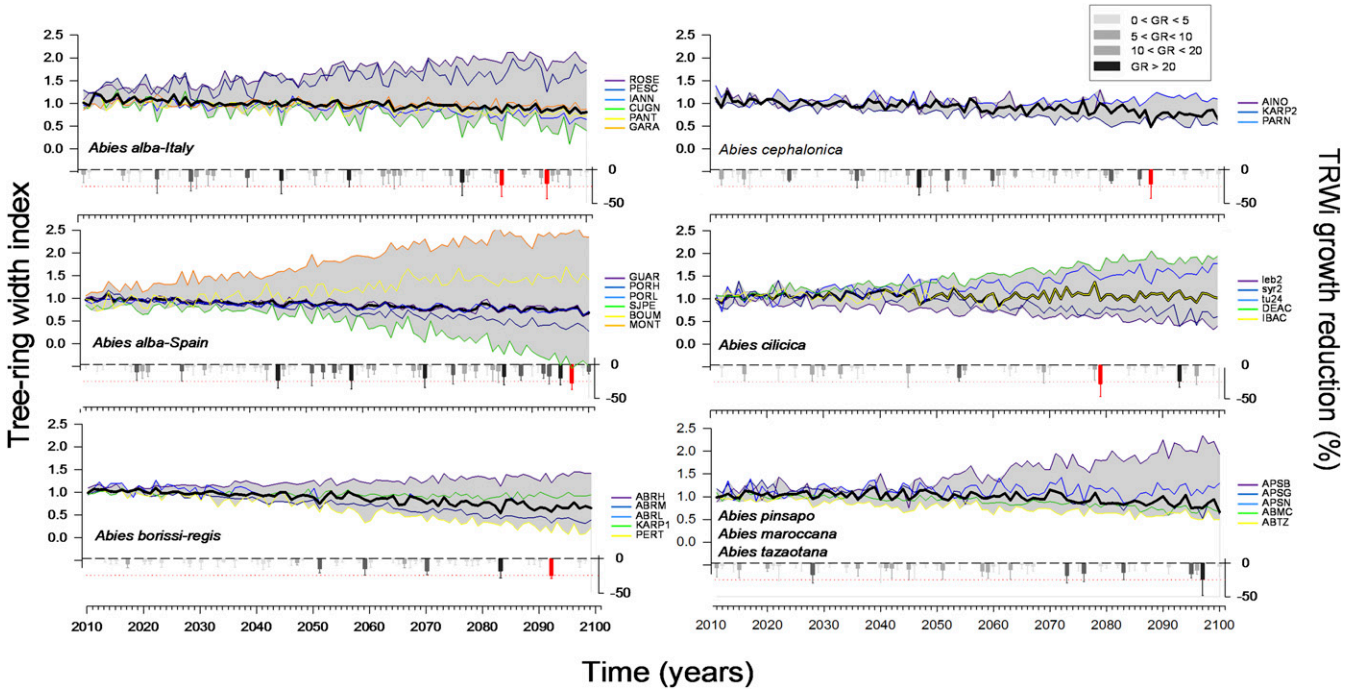

Fig. 2. Projected ring-width indices (TRWi) for each fir species and site considering the warmest emission scenario (RCP 8.5). Species climate-based models means are shown as black lines, and gray areas represent the maximum and minimum TRWi values considering all sites for each species. The lower plots of each panel show the assessment of the impact on growth stability (sensitivity) of the occurrence of extreme forecasted 21st-century events by TRWi reductions (GR) computed considering the 5-y moving average values from 2011 to 2100. The gray-scale bars indicate TRWi reductions while red bars indicate selected climatically extreme years causing reduced growth in each species during the 21st century. Bold lines frame extreme values (TRWi reduction >25%). See *SI Appendix*, Fig. S5, for RCP 4.5 scenario and *SI Appendix*, Table S1, for site codes.

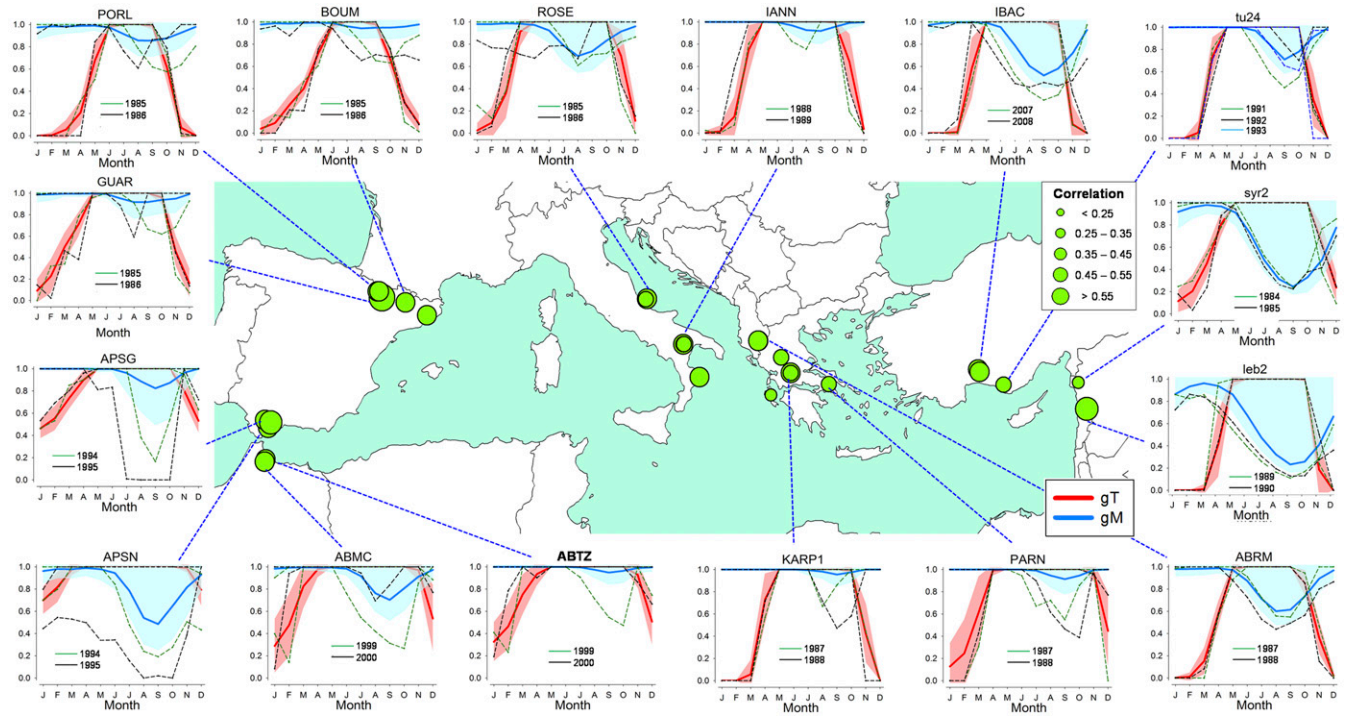

Fig. 3. Simulated monthly growth response curves (*gT*, *gM*) using the VS-Lite model for the period 1950–2010. The growth responses consider temperature (*gT*, red lines and red areas correspond to the mean and SD, respectively) and soil moisture limitations (*gM*, blue lines and blue areas correspond to the mean and SD, respectively) for each species. See Fig. 1 and *SI Appendix*, Table S1, for site codes. Note that low-*gM* values indicate growth limitations. Selected extremely low growth years are indicated by dashed lines in different colors: green (previous year) and black (current year). The map displays site-level Pearson correlation coefficients computed by the VS-Lite growth model between observed and predicted series of ring-width indices. See *SI Appendix*, Fig. S7, for more locations.

closure of stomata that provides an efficient reduction of water loss in the case of water shortage (46, 47). However, as already observed, the loss in hydraulic performance during extreme events can translate into growth decline (19), especially given that high temperatures in combination with strong radiation can also negatively influence soil water balance (48). Unexpectedly, the highest vulnerability of fir species is recorded on soils with higher water-holding capacity, showing that soil features need to be explicitly considered to properly assess tree vulnerability and growth potential (49). For example, the strict water-stress avoidance strategy of *A. pinsapo* and *A. cephalonica* to limit water losses is reflected in rapid stomatal closure at rather positive stem water potentials and relatively high values of soil water content (15, 47).

Stability of Climate Refugia Under Different Warming Scenarios. Under the strongest temperature increases, the VS-lite growth model projected population shifts from moisture-limited to also warming-limited conditions during the growing season (Figs. 3 and 4). This would occur mainly in lower and dry sites where spring–summer conditions are presently close to the species' limits (Fig. 5) and where the future climate will be similar to current extreme (drought/heat spells) events (Figs. 3 and 5). In general, climate projections predict shorter growing seasons in southern *A. alba* and lower elevation *A. borisii-regis*, *A. cephalonica*, *A. cilicica*, and *A. pinsapo* sites, but longer ones in the wettest and high-elevation *A. alba* sites (25) (Figs. 3 and 4). This would imply a higher growth sensitivity to climate during the early growing season, suggesting a prominent role of spring water deficit as already observed in xylogenesis investigations (50). On the contrary, the minimum temperature threshold for growth (T_1) and the temperature at which growth is not limited (T_2) will increase for all CMFF (*SI Appendix*, Tables S4 and S7), with a potential increased frequency of evapotranspiration stress during the predicted shorter growing season (Fig. 5) (4). Thus, the forecasted drier and hotter growing season would negatively affect the growth of CMFF stands at lower elevation and xeric sites by exceeding their functional thresholds for optimal growth responses (i.e., *gT* and *gM*) (Figs. 4 and 5).

Since all of the CMFF experienced a fairly stable thermal range during most of the Holocene (51), an increase in water and thermal stress during the second half of the 21st century may have dreadful effects on the relict populations at the warm (lower) edges of the species' ranges (Fig. 5). Assuming a low genetic variability within these species (see ref. 52), few fir taxa may potentially withstand a temperature increase of about 4.8 °C in xeric sites (Fig. 4). Our results thus suggest that some of the quaternary populations' refugia at the warmer end of the species distribution (e.g., *A. pinsapo*, *A. tazaotana*, or low elevation *A. cephalonica* and *A. cilicica*) may be threatened within a climate warming scenario (Fig. 5 and *SI Appendix*, Table S7).

Evaluating the climatic limits of species distributions over time is key to understanding the species responses to future climate change. Space–time extended datasets, such as those derived from tree rings, are needed to reconstruct species resilience to past extreme events and to predict future dieback processes (cf. 18 and 53). Our methodological framework is robust and provides results that are in accordance with what has been observed in field studies on forest vulnerability and climate-driven growth thresholds (15, 19). Nevertheless, we captured only part of the key drivers governing forest growth, and future simulations should also include information on shoot and leaf growth (54), demographic processes (55), and tree acclimation and disturbances (56).

Conclusions. Our modeling approach helps to highlight locally resistant tree populations, providing drought-heat tolerance that can be potentially preadapted to future climatic conditions expected in more northerly locations. Having these sources for assisted migration can be highly relevant for the application of conservation strategies under global change or habitat fragmentation. Finally,

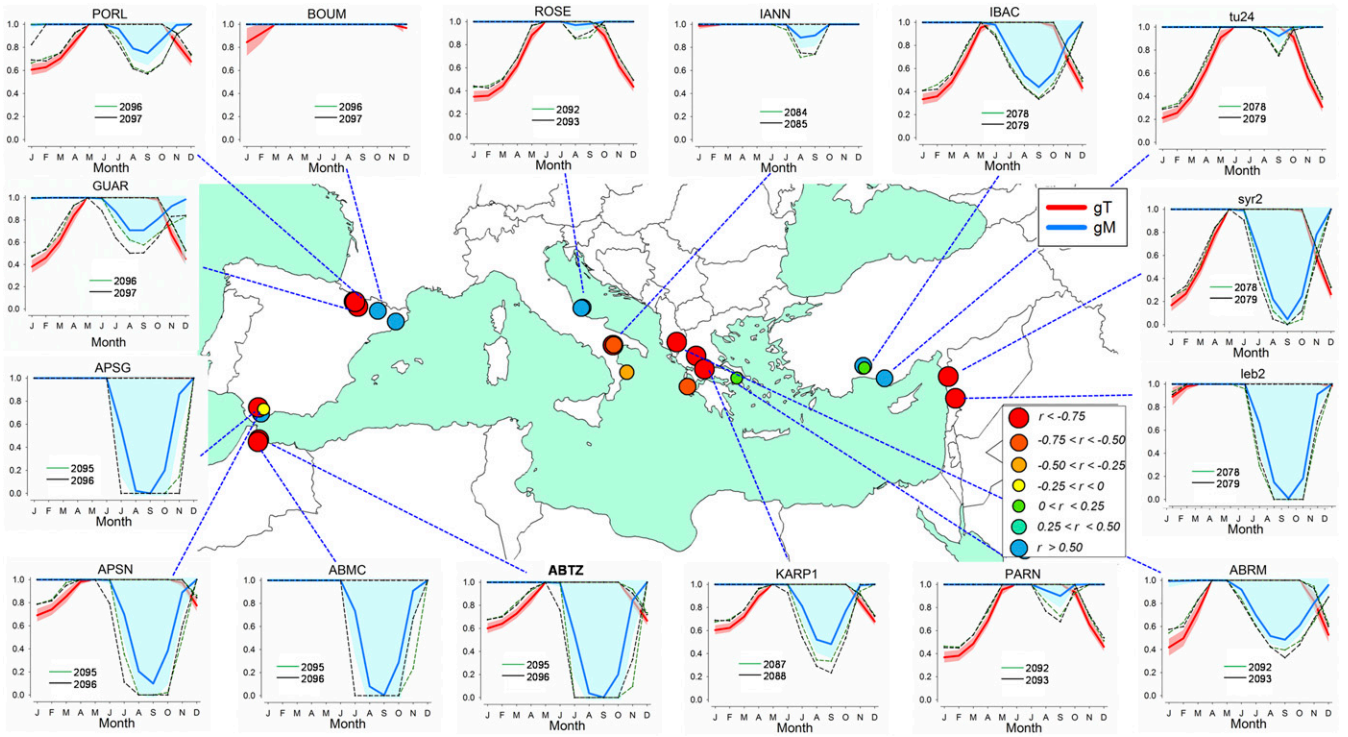

Fig. 4. Projected monthly growth response curves using VS-Lite model for the 2050–2100 period under the RCP 8.5 scenario. The response curves consider temperature (*gT*, red lines and red areas correspond to the mean and SD, respectively) and soil moisture limitations (*gM*, blue lines and blue areas correspond to the mean and SD, respectively) for each site (Fig. 1). Selected extreme low growth years are indicated by dashed lines in different colors: green (previous year) and black (current year) (Fig. 2 and *SI Appendix*, Fig. S5). The map symbols show projected growth trends (Pearson correlation coefficients of site mean TRWi series) considering the 2011–2100 period following growth projections (*SI Appendix*, Table S2). Correlation values higher than |0.25| are significant at $P < 0.05$. See *SI Appendix*, Table S1 for site codes and *SI Appendix*, Fig. S8, for more locations.

growth analyses should be ideally supplemented by the genetic background of the species when stakeholders have to decide about management but also to confer resilience to forests. Process-based models allowed us to define the vulnerability thresholds of CMFF refugia by quantifying growth responses and identifying vulnerability thresholds to forecasted climate warming and more extreme dry spells (Fig. 1). We disentangled the respective roles of the different species- and site-specific factors that will predispose to growth decline and local extinction processes. The predictions under the business-as-usual scenario (RCP 8.5) forecasted a growth reduction in some southern forests. This knowledge can support forest managers to better prepare specific strategies to cope with forecasted climatic challenges.

Materials and Methods

Study Sites and Sampling Design. The study area includes the main ranges of most Circum-Mediterranean fir (*Abies*) species (CMFF) (*SI Appendix*, Fig. S1 and Table S1) (11). Fir species appear in the wettest sites of the Mediterranean Basin usually dominating in *N*-oriented sites with deep soils (57). They can be found on different parent materials, calcareous or noncalcareous, but grow best on deeper acid soils with high water reserves (15). These species develop in a subhumid climate where annual precipitation is between 600 and 1,000 mm, and mean annual temperature ranges from 6.6 to 17.2 °C (*SI Appendix*, Table S5).

Thirty forests that were sampled across the Mediterranean region are distributed as follows: *A. alba* Miller, six sites in Italy (58), six sites in Spain (25); *A. borisii-regis* Mattfeld (five sites) (41, 48); *A. cephalonica* Loudon (three sites) (38, 41); *A. cilicica* (Antoine and Kotschy) Carrière (five sites); *A. pinsapo* Boissier (three sites); *A. pinsapo* var. *maroccana* (Trabut) Ceballos and Bolaños (one site); and *A. pinsapo* var. *tazaotana* (Cózar ex Huguet del Villar) Pourtet (one site) (*SI Appendix*, Fig. S1 and Table S1). We sampled these sites following dendrochronological methods and covering most of the geographical distribution of *Abies* species in the Mediterranean, thus capturing most of the ecological variability experienced by these species (*SI Appendix*, Fig. S1) (15). Most sampled sites are in protected areas (e.g., national parks), which guarantee that trees have been less exposed to disturbances (e.g., logging or fire) than in nonprotected areas at least for the past 50–60 y. At each site, at least 12 dominant or codominant trees (when they were available) separated by at least 20 m from each other were cored at 1.3 m using Pressler increment borers on the cross-slope sides of the trunk whenever possible. For each study site, latitude, longitude, and mean elevation as well as topographic (slope and aspect) variables were recorded (*SI Appendix*, Table S1). Radial growth was measured in two to three radial cores per tree. Wood samples were sanded until rings were visible and then visually cross-dated. Once dated, tree-ring widths were measured to the nearest 0.01 mm using a binocular microscope and a LINTAB measuring device (Rinntech). The accuracy of visual cross-dating and measurements was checked with the COFECHA program, which calculates moving correlations between each individual tree-ring series and the mean site series (59).

Climate-Growth Associations. The homogenized and quality-checked CRU T.S. 3.23 dataset (www.cru.uea.ac.uk/data) was used for the period 1950–2010, providing a reliable climate data source across all of the study sites (60). This dataset contains monthly mean temperature and precipitation data gridded at a 0.5° spatial resolution that have been checked for homogeneity.

To quantify climate-growth associations, we calculated mean tree-ring width series at the site scale (site chronology) (*SI Appendix*, Table S1). TRWi were calculated, adjusting negative exponential or linear functions and 30-y-long splines to obtain detrended growth series and corrected age–size trends. These splines allowed high-frequency (annual to decadal) growth variability to be preserved. We applied autoregressive models to model and eliminate most of the temporal (usually of first order) autocorrelation. We obtained residual or prewhitened TRWi series for each tree as ratios between the measurement and the fitted curve. Finally, we averaged the individual growth-index series into site-level chronologies following a hierarchical approach from tree to site. Among the developed chronologies, we considered only those covering the period 1950–2010, which corresponded to the period of most reliable climate data in the study area. To characterize these site TRWi chronologies, we also calculated several dendrochronological statistics (*SI Appendix*, Table S1) (61).

The relationships between monthly climate data (mean temperatures and precipitation) and TRWi were assessed by calculating bootstrapped Pearson

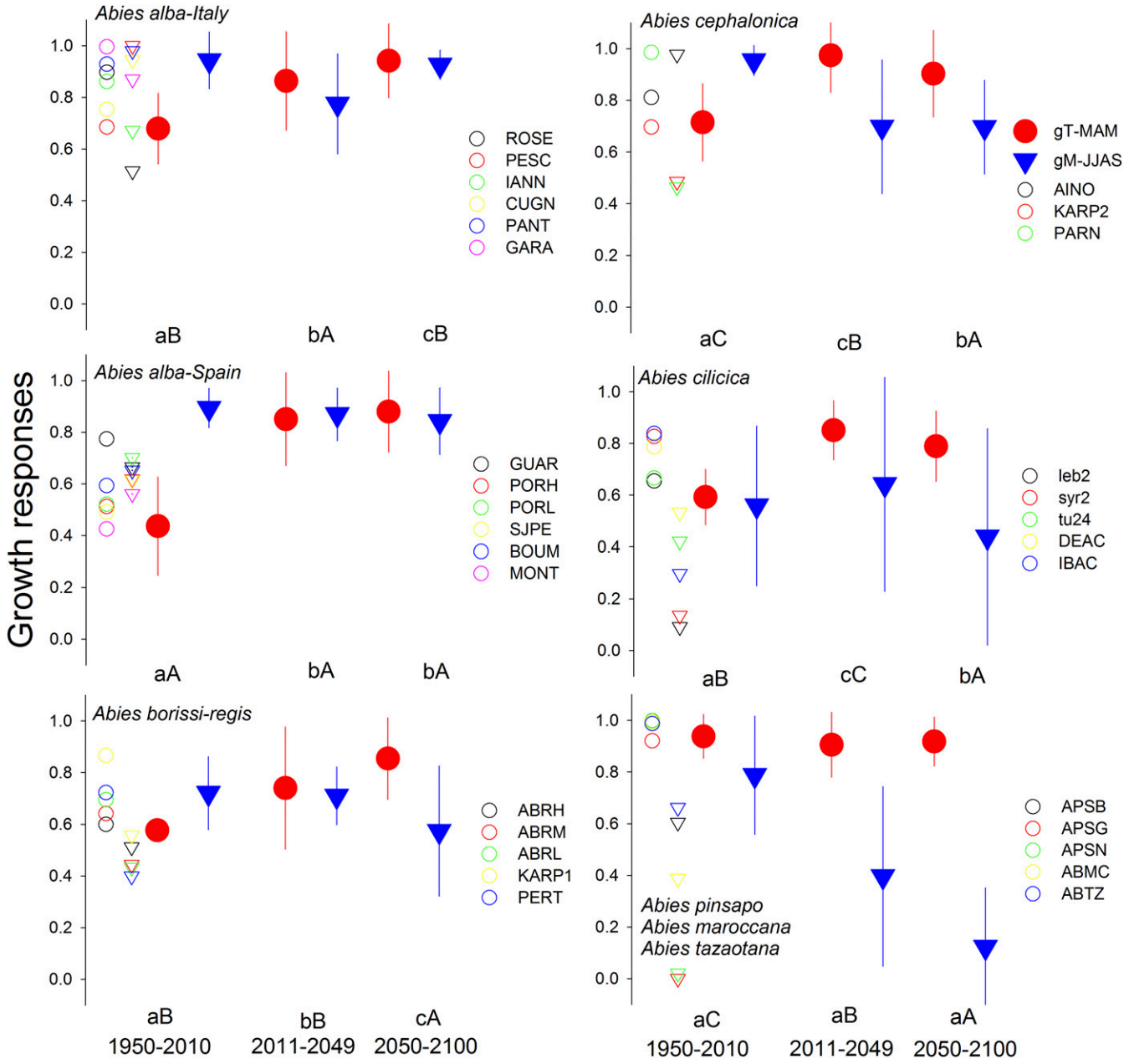

Fig. 5. Simulated (VS-Lite model) mean growth responses for the growing season and climate extreme years. The selected periods represent spring (March to May) temperature (*gT*, red circles indicate the mean and SD) and summer (June to September) soil moisture limitations (*gM*, blue triangles indicate the mean and SD) for each *Abies* species. See *SI Appendix*, Fig. S9 and Table S1 for site codes. Values were fitted for one observed (1950–2010) and two projected 21st-century periods (2011–2049 and 2050–2100) based on RCP 8.5 emission scenario. Selected observed growth responses during extreme events (1950–2010 period; see Figs. 1–3) with extremely low growth rates are indicated in different colors on the *Left* for each site. See also Figs. 2 and 3. These values defined the observed thresholds of vulnerability for each climate refugia compared with the forecasted growth response for the RCP 8.5 climate scenario. Different letters indicate significant ($P < 0.05$) differences between observed and projected periods based on Tukey's HSD post hoc tests (lowercase and uppercase letters correspond to the 2011–2049 and 2050–2100 periods, respectively).

correlation coefficients for the common period 1950–2010. The temporal window of growth-climate comparisons included from the previous September to the current October. All stages of chronologies building and further analyses were performed using the *R* statistical software (62) and the package *dplR* (63). This first step of our conceptual framework defines the critical growing period at site and species levels and which climate variables (i.e., monthly temperature and precipitation) affect growth (Fig. 1).

Climate Extremes and Pointer Years. As the term "climate extreme" usually defines both "extreme weather" and "extreme climate" events (cf. 63), we considered 27 climate indices (11 for precipitation and 16 for temperature) from daily observations of precipitation and maximum and minimum temperature (ETCCDI database) calculated for each site by using the RClimDex package (see etccdi.pacificclimate.org/indices_def.shtml and *SI Appendix*, Table S8). RClimDex was used to compute climate indices from the observed and forecasted ensemble climate data (65–67). Spearman correlation coefficients were calculated for each site between TRWi and annual climate indices considering the previous and current year of tree-ring formation. This allowed the presence of any carryover effect of climate extremes to the following tree-ring formation to be assessed (*SI Appendix*, Table S9) (68).

Vulnerability to climate change during these extreme climate events was assessed using extreme pointer year analysis. This was performed to determine

whether climatic factors were responsible for conspicuously narrower or wider tree rings as described in ref. 69 (Fig. 1). Species- and site-specific pointer years were calculated on raw annual ring-width values for each tree and were then transformed into normalized values (Cropper index). This method z-transforms tree growth in year *i* within a symmetric moving window of *n* years (5 y in our case), thereby providing the number of SDs of tree growth in individual years from the window average (70). To calculate the intensity of interannual growth anomalies, we defined the probability density functions of the standardized normal distribution of data (see ref. 71) and identified the strong negative growth anomalies during extreme events. The resulting time series of normalized values allowed for the interpretation of the growth characteristics under extreme events in terms of yearly SD units for each tree, site, and species. Cropper values were then normalized to a mean of 0 and an SD of 1. To evaluate the probability of a strong negative growth anomaly, threshold values were defined as follows: "extreme": > 1.64; "strong": > 1.28; and "weak" > 1; values between −1 and +1 were considered as "normal" (see ref. 71). The weak threshold value was used to maximize the number of years for further analyses. When more than 50% of all trees within a chronology exceeded the defined threshold, the year was considered a pointer year (69).

To assess the impact on growth (sensitivity) of the occurrence of pointer years, we also calculated the annual percentage of growth change (GC) of each tree by calculating the ratio of tree growth in year *i* and the average growth of the 5 preceding years. To assess the tree response to 21st-century impact on forecasted growth trends, the TRWi reduction (GR: the ratio of TRWi in year *i* and the average TRWi of 5 preceding years) was also calculated for each tree. To calculate the pointer years and the GC components, we used the pointRes package (72).

Climate Projections. Only those climate variables highly correlated with TRWi ($r > |0.30|$, $P < 0.05$) were considered in the climate-based models and TRWi projections under different climate scenarios. The climate data projected for the 21st century were downloaded and downscaled (cf. 72) at a 0.5° spatial resolution from the fifth phase of the Coupled Model Intercomparison Project (ensemble CMIP5) (74). We used data for the scenario (RCP 8.5) that most closely tracked recent historical emissions (75), and one lower-emission scenario (RCP 4.5) in which the increase in annual emissions is more gradual during the early 21st century and declines after the mid-21st century. These scenarios result in 1.7–4.8 °C global warming by the year 2100, relative to the late–20th-century baseline. The RCP 4.5 scenario represents a situation where radiative forcing peaks at 4.5 $W{\cdot}m^{-2}$ after 2100 with temperature increases ranging between 0.9 and 2.6 °C during the 21st century, whereas in the RCP 8.5 scenario radiative forcing continuously rises to reach 8.5 $W{\cdot}m^{-2}$ in 2100 with a warming increase ranging between 1.4 and 4.8 °C (26).

Growth Projections Based on Process-Based Modeling of Tree Growth. We used the VS-Lite model and a Bayesian parameter estimation approach to simulate TRWi as a function of climate (Fig. 1) (76–78). The model uses the Leaky Bucket Model of hydrology provided by the National Oceanic and Atmospheric Administration Climate Prediction Center (79) to estimate monthly soil moisture from temperature and total precipitation data. Snow dynamics are not explicitly considered in the model, and thus all precipitation is assumed to be liquid. For each year, the model simulates standardized tree-ring width anomalies from the minimum of the monthly growth responses to temperature (*gT*) and moisture (*gM*), modulated by insolation (*gE*). Day length is determined from site latitude and does not vary from year to year. The growth response functions for temperature (*gT*) and moisture (*gM*) in VS-Lite involve only two parameters. The first represents the temperature (T_1) or moisture (M_1) threshold below which growth will not occur, while the second is the optimal temperature (T_2) or moisture (M_2) above which growth is not limited by climate (Fig. 1). The growth function parameters were estimated for each site via Bayesian calibration. This scheme assumes uniform priors for the growth response parameters and independent, normally distributed errors for the modeled TRWi values. The posterior median for each parameter was used to obtain the "calibrated" growth response for a given site. Finally, the model was run over the entire period 1950–2010 using the calibrated parameters for each site to produce a simulated tree-ring chronology ($TRWi_{VSL}$) that represents an estimate of the site climate signal of forest growth. A more detailed description of the approach can be found in ref. 78.

Temperature (T_i) and soil moisture (M_i) growth parameters were sampled uniformly across intervals, and the growth parameter set producing the simulation that correlated most significantly with the corresponding observed TRWi series for each site was then used in the simulations. In addition, other parameters (e.g., soil moisture, runoff, root depth) were taken from published studies (25, 76–82). The model was evaluated 10,000 times for each site using three parallel Markov Chain Monte Carlo chains with uniform prior distribution for each parameter and a white Gaussian noise model error (78). To compute annual TRWi values, we integrated the overall simulated growth rates (i.e., the point-wise minimum of monthly *gT*, *gM*, and *gE*) over the time window from September of the year before growth to October of the year of tree-ring formation. This period was determined following previous xylogenesis and dendroecological studies performed on these species (15, 41, 50, 83). To evaluate the temporal stability of the calibrated growth response functions, we divided the period 1950–2010 into two 30-y intervals (1950–1980, 1980–2010) and withheld the second half for validation of the parameters estimated in the first half.

Climate-growth relationships were reexamined by applying stepwise multiple linear regressions. This allowed the effects of climate and extreme indices in the observed TRWi data to be identified and to project TRWi through individual-site climate-based equations under future scenarios (Fig. 1). All continuous predictor variables were standardized to give them the same weight in the fitted models (i.e., the mean was subtracted from each value and divided by the SD), enabling the interactions to be tested and compared (84). In addition, we evaluated the existence of multicollinearity among explanatory variables by calculating the variance inflation factor, which, being lower than 2, confirmed no redundancy problems with the data. We used the function "step" of the R package "stats" (62) using the lowest Akaike Information Criterion to select the final regression equations. The models were fitted using Generalized Least-Squares estimation and the R package "nlme" (85). The selected models were run to forecast the TRWi of each site (hereafter, $TRWi_p$) for the 2011–2049 and 2050–2100 periods under the two selected RCP scenarios. Finally, we ran VS-Lite models on the $TRWi_p$ series over the same periods to forecast growth responses (i.e., *gT*, *gM*) and growth function parameters (T_1, T_2 and M_1, M_2) under future climate projections (see above).

Vulnerability of Mediterranean Firs. To explore the stability of Mediterranean *Abies* refugia under different forcing climate scenarios, we compared the observed and forecasted growth responses to temperature (*gT*) and soil moisture (*gM*) for the 2011–2049 and 2050–2100 periods under the RCP scenarios (Fig. 1). We did this by analyzing the growth projections of each site climate-based model including Extreme Climate Indices (86). All forecasted values exceeding at least two SDs of the observed mean growth response (*gT*, *gM*) during the growing season were defined as vulnerable climate refugia; i.e., refugia exposed to a highly elevated climate instability (87). We chose the growth responses to observed extreme climate events to declare vulnerability since drought- or heat-induced forest dieback episodes have already been documented in response to heat waves and dry spells in several Mediterranean fir species, particularly in the case of Silver fir (*A. alba*) and Spanish fir (*A. pinsapo*) (13, 20, 36, 40, 83).

ACKNOWLEDGMENTS. We thank the Climatic Research Unit for providing the climate databases used in this study; Dr. Geert Jan van Oldenborgh for assistance; the contributors to the International Tree-Ring Data Bank; José B. López-Quintanilla, José L. Sánchez Vallejo, Francisco Jarillo, José Ramón Guzmán Álvarez, and Fernando Ríos (Consejería de Medio Ambiente y Ordenación del Territorio, Junta de Andalucía); Miguel Sánchez González and Pedro Salguero Fernández for their support during fieldwork; and useful comments provided by K. Seftigen. A special thanks for the great efforts made by our late colleague, Fernando Molina Vázquez. R.S.-S. is supported by Postdoctoral Grant IJCI-2015-25845 (Fondo Europeo de Desarrollo Regional funds). This study was supported by projects 387/2011 (Organismo Autónomo de Parques Nacionales, Spanish Ministry of Environment), CGL2011-26654; FunDiver (CGL2015-69186-C2-1-R); CoMo-ReAdapt (CGL2013-48843-C2-1-R) (Spanish Ministry of Economy); and Cambio Climático y Adaptación de los Bosques del Pirineo (CANOPEE) (Interreg V-A POCTEFA 2014-2020-Fondo Europeo de Desarrollo Regional funds).

1. Davis MB, Shaw RG (2001) Range shifts and adaptive responses to Quaternary climate change. *Science* 292:673–679.
2. IPCC (2013) *Climate Change 2013: The Physical Science Basis. Contribution of Working Group I to the Fifth Assessment Report of the Intergovernmental Panel on Climate Change*, eds Stocker TF, et al. (Cambridge Univ Press, Cambridge, UK).
3. Hampe A, Jump AS (2011) Climate relicts: Past, present, future. *Annu Rev Ecol Evol Syst* 42:313–333.
4. Allen CD, Breshears DD, McDowell NG (2015) On underestimation of global vulnerability to tree mortality and forest die-off from hotter drought in the Anthropocene. *Ecosphere* 6:1–55.
5. Anderegg WRL, Kane J, Anderegg LDL (2013) Consequences of widespread tree mortality triggered by drought and temperature stress. *Nat Clim Chang* 3:30–36.
6. Nicotra AB, et al. (2010) Plant phenotypic plasticity in a changing climate. *Trends Plant Sci* 15:684–692.

7. Tzedakis PC, Lawson IT, Frogley MR, Hewitt GM, Preece RC (2002) Buffered tree population changes in a quaternary refugium: Evolutionary implications. *Science* 297: 2044–2047.
8. Linares JC, Delgado-Huertas A, Carreira JA (2011) Climatic trends and different drought adaptive capacity and vulnerability in a mixed *Abies pinsapo - Pinus halepensis* forest. *Clim Change* 105:67–90.
9. Seneviratne SI, Donat MG, Pitman AJ, Knutti R, Wilby RL (2016) Allowable CO_2 emissions based on regional and impact-related climate targets. *Nature* 529:477–483.
10. Hampe A, Rodríguez-Sánchez F, Dobrowski S, Hu FS, Gavin DG (2013) Climate refugia: From the last glacial maximum to the twenty-first century. *New Phytol* 197:16–18.
11. Linares JC (2011) Biogeography and evolution of *Abies* (Pinaceae) in the Mediterranean Basin. The roles of long-term climatic changes and glacial refugia. *J Biogeogr* 38: 619–630.
12. Linares JC, Carreira JA (2009) Temperate-like stand dynamics in relict Mediterranean-fir (*Abies pinsapo* Boiss.) forests from Southern Spain. *Ann For Sci* 66:610.
13. Linares JC, Carreira JA, Ochoa V (2011) Human impacts drive forest structure and diversity. Insights from Mediterranean mountain forest dominated by Abies pinsapo. *Eur J For Res* 130:533–542.
14. Tinner W, et al. (2013) The past ecology of *Abies alba* provides new perspectives on future responses of silver fir forests to global warming. *Ecol Monogr* 83:419–439.
15. Aussenac G (2002) Ecology and ecophysiology of circum-Mediterranean firs in the context of climate change. *Ann For Sci* 59:823–832.
16. Bigler C, Bugmann H (2004) Predicting the time of tree death using dendrochronological data. *Ecol Appl* 14:902–914.
17. Bigler C, Bräker OU, Bugmann H, Dobbertin M, Rigling A (2006) Drought as an inciting mortality factor in Scots pine stands of the Valais, Switzerland. *Ecosystems (N Y)* 9:330–343.
18. Williams A, et al. (2013) Temperature as a potent driver of regional forest drought stress and tree mortality. *Nat Clim Chang* 3:292–297.
19. Camarero JJ, Gazol A, Sangüesa-Barreda G, Oliva J, Vicente-Serrano SM (2015) To die or not to die: Early-warning signals of dieback in response to a severe drought. *J Ecol* 103:44–57.
20. Cailleret M, et al. (2017) A synthesis of radial growth patterns preceding tree mortality. *Glob Change Biol* 23:1675–1690.
21. García-Valdés R, Zavala MA, Araújo MB, Purves DW (2013) Chasing a moving target: Projecting climate change-induced shifts in non-equilibrial tree species distributions. *J Ecol* 101:441–453.
22. García-Valdés R, Gotelli NJ, Zavala MA, Purves DW, Araújo MB (2015) Effects of climate, species interactions, and dispersal on decadal colonization and extinction rates of Iberian tree species. *Ecol Modell* 309:118–127.
23. Talluto MV, Boulangeat I, Vissault S, Thuiller W, Gravel D (2017) Extinction debt and colonization credit delay range shifts of eastern North American trees. *Nat Ecol Evol* 1:0182.
24. Zhang J, et al. (2017) Extinction risk of North American seed plants elevated by climate and land-use. *J Appl Ecol* 54:303–312.
25. Sánchez-Salguero R, et al. (2017) Assessing forest vulnerability to climate warming using a process-based model of tree growth: Bad prospects for rear-edges. *Glob Change Biol* 23:2705–2719.
26. van Vuuren DP, et al. (2011) The representative concentration pathways: An overview. *Clim Change* 109:5–31.
27. Vaganov EA, Hughes MK, Shashkin AV (2006) *Growth Dynamics of Conifer Tree Rings* (Springer, Berlin).
28. Vaganov EA, Anchukaitis KJ, Evans MN (2011) How well understood are the processes that create dendroclimatic records? A mechanistic model of the climatic control on conifer tree-ring growth dynamics. *Dendroclimatology,* Developments in Paleoenvironmental Research, eds Hughes MK, Swetnam TW, Diaz HF (Springer, Dordrecht, The Netherlands), pp 37–75.
29. Hampe A, Petit RJ (2005) Conserving biodiversity under climate change: The rear edge matters. *Ecol Lett* 8:461–467.
30. Dawson TP, Jackson ST, House JI, Prentice IC, Mace GM (2011) Beyond predictions: Biodiversity conservation in a changing climate. *Science* 332:53–58.
31. Rogers BM, Jantz P, Goetz SJ (2017) Vulnerability of eastern US tree species to climate change. *Glob Change Biol* 23:3302–3320.
32. Ruosch M, et al. (2016) Past and future evolution of *Abies alba* forests in Europe - comparison of a dynamic vegetation model with palaeo data and observations. *Glob Change Biol* 22:727–740.
33. Büntgen U, et al. (2014) Placing unprecedented recent fir growth in a European-wide and Holocene-long context. *Front Ecol Environ* 12:100–106.
34. Gazol A, et al. (2015) Distinct effects of climate warming on populations of silver fir (*Abies alba*) across Europe. *J Biogeogr* 42:1150–1162.
35. McDowell N, et al. (2008) Mechanisms of plant survival and mortality during drought: Why do some plants survive while others succumb to drought? *New Phytol* 178: 719–739.
36. Camarero JJ, Bigler C, Linares JC, Gil-Pelegrin E (2011) Synergistic effects of past historical logging and drought on the decline of Pyrenean silver fir forests. *For Ecol Manage* 262:759–769.
37. Anderegg WRL, et al. (2012) The roles of hydraulic and carbon stress in a widespread climate-induced forest die-off. *Proc Natl Acad Sci USA* 109:233–237.
38. Koutavas A (2013) CO_2 fertilization and enhanced drought resistance in Greek firs from Cephalonia Island, Greece. *Glob Change Biol* 19:529–539.
39. Peñuelas J, Hunt JM, Ogaya R, Jump AS (2008) Twentieth century changes of tree-ring delta C-13 at the southern range-edge of *Fagus sylvatica*: Increasing water-use efficiency does not avoid the growth decline induced by warming at low altitudes. *Glob Change Biol* 14:1076–1088.
40. Linares JC, Camarero JJ (2012) From pattern to process: Linking intrinsic water-use efficiency to drought-induced forest decline. *Glob Change Biol* 18:1000–1015.
41. Papadopoulos AM (2016) Tree-ring patterns and climate response of Mediterranean fir populations in Central Greece. *Dendrochronologia* 40:17–25.
42. Rolland C (1993) Tree-ring and climate relationships for *Abies alba* in the internal Alps. *Tree-Ring Bull* 53:1–11.
43. Adams HD, et al. (2009) Temperature sensitivity of drought-induced tree mortality portends increased regional die-off under global-change-type drought. *Proc Natl Acad Sci USA* 106:7063–7066.
44. George JP, et al. (2015) Inter- and intra-specific variation in drought sensitivity in Abies spec. and its relation to wood density and growth traits. *Agric Meteorol* 214-215:430–443.
45. Valladares F, et al. (2014) The effects of phenotypic plasticity and local adaptation on forecasts of species range shifts under climate change. *Ecol Lett* 17:1351–1364.
46. Peguero-Pina JJ, et al. (2011) Hydraulic traits are associated with the distribution range of two closely related Mediterranean firs, *Abies alba* Mill. and Abies pinsapo Boiss. *Tree Physiol* 31:1067–1075.
47. Sánchez-Salguero R, et al. (2015) Regulation of water use in the southernmost European fir (*Abies pinsapo* Boiss.): Drought avoidance matters. *Forests* 6:2241–2260.
48. Pasho E, Toromani E, Allan AQ (2014) Climatic impact on tree-ring widths in *Abies borisii-regis* forests from South-East Albania. *Dendrochronologia* 32:237–244.
49. Nourtier M, et al. (2014) Transpiration of silver Fir (*Abies alba* Mill.) during and after drought in relation to soil properties in a Mediterranean mountain area. *Ann Sci* 71: 683–695.
50. Cuny HE, Rathgeber CBK, Lebourgeois F, Fortin M, Fournier M (2012) Life strategies in intra-annual dynamics of wood formation: Example of three conifer species in a temperate forest in north-east France. *Tree Physiol* 32:612–625.
51. Cheddadi R, et al. (2016) Temperature range shifts for three European tree species over the last 10,000 years. *Front Plant Sci* 7:1581.
52. Sánchez-Robles JM, et al. (2014) Phylogeography of SW Mediterranean firs: Different European origins for the North African *Abies* species. *Mol Phylogenet Evol* 79:42–53.
53. Pecl GT, et al. (2017) Biodiversity redistribution under climate change: Impacts on ecosystems and human well-being. *Science* 355:1389.
54. Vitasse Y, et al. (2011) Assessing the effects of climate change on the phenology of European temperate trees. *Agric Meteorol* 151:969–980.
55. Matías L, Jump AS (2015) Asymmetric changes of growth and reproductive investment herald altitudinal and latitudinal range shifts of two woody species. *Glob Change Biol* 21:882–896.
56. Millar CI, Stephenson NL (2015) Temperate forest health in an era of emerging megadisturbance. *Science* 349:823–826.
57. Caudullo G, Tinner W (2016) *Abies*–Circum-Mediterranean firs in Europe: Distribution, habitat, usage and threats. *European Atlas of Forest Tree Species*, eds San-Miguel-Ayanz J, de Rigo D, Caudullo G, Houston Durrant T, Mauri A (Publications Office of the European Union, Luxembourg).
58. Carrer M, Nola P, Motta R, Urbinati R (2010) Contrasting tree-ring growth to climate responses of Abies alba toward the southern limit of its distribution area. *Oikos* 119: 1515–1525.
59. Grissino-Mayer HD (2001) Evaluating crossdating accuracy: A manual and tutorial for the computer program COFECHA. *Tree-Ring Res* 57:205–221.
60. Harris I, Jones PD, Osborn TJ, Lister DH (2014) Updated high-resolution grids of monthly climatic observations: The CRU TS3.10 Dataset. *Int J Climatol* 34:623–642.
61. Wigley TML, Briffa KR, Jones PD (1984) On the average value of correlated time series, with applications in dendroclimatology and hydrometeorology. *J Clim* 23:201–213.
62. R Development Core Team (2017) R: A Language and Environment for Statistical Computing (R Foundation for Statistical Computing, Vienna), Version 3.3.3. Available at www.r-project.org/. Accessed March 30, 2017.
63. Bunn AG (2010) Statistical and visual crossdating in R using the *dplR* library. *Dendrochronologia* 28:251–258.
64. Frank D, et al. (2015) Effects of climate extremes on the terrestrial carbon cycle: Concepts, processes and potential future impacts. *Glob Change Biol* 21:2861–2880.
65. Donat MG, et al. (2013) Updated analyses of temperature and precipitation extreme indices since the beginning of the twentieth century: The HadEX2 dataset. *J Geophys Res Atmos* 118:2098–2118.
66. Sillmann J, Kharin VV, Zhang X, Zwiers FW, Bronaugh D (2013) Climate extremes indices in the CMIP5 multimodel ensemble: I. Model evaluation in the present climate. *J Geophys Res* 118:1716–1733.
67. Sillmann J, Kharin VV, Zwiers FW, Zhang X, Bronaugh D (2013) Climate extremes indices in the CMIP5 multimodel ensemble: II. Future climate projections. *J Geophys Res* 118:2473–2493.
68. Cook ER, Kairiukstis LA (1990) *Methods of Dendrochronology: Applications in the Environmental Sciences* (Kluwer Academic Publishers, International Institute for Applied Systems Analysis, Dordrecht, The Netherlands).
69. Schweingruber FH, Eckstein D, Bachet S, Bräker OU (1990) Identification, presentation and interpretation of event years and pointer years in dendrochronology. *Dendrochronologia* 8:9–38.
70. Cropper JP (1979) Tree ring skeleton plotting by computer. *Tree-Ring Bull* 39:47–60.
71. Neuwirth B, Schweingruber FH, Winiger M (2007) Spatial patterns of central European pointer years from 1901 to 1971. *Dendrochronologia* 24:79–89.
72. van der Maaten-Theunissen M, van der Maaten E, Bouriaud O (2015) pointRes: An R package to analyze pointer years and components of resilience. *Dendrochronologia* 35:34–38.
73. Moreno A, Hasenauer H (2016) Spatial downscaling of European climate data. *Int J Climatol* 36:1444–1458.
74. Taylor KE, Stouffer RJ, Meehl GA (2012) An overview of CMIP5 and the experiment design. *Bull Am Meteorol Soc* 93:485–498.

75. Lelieveld J, et al. (2016) Strongly increasing heat extremes in the Middle East and North Africa (MENA) in the 21st century. *Clim Change* 137:245–260.
76. Tolwinski-Ward SE, Tingley MP, Evans MN, Hughes MK, Nychka DW (2015) Probabilistic reconstructions of local temperature and soil moisture from tree-ring data with potentially time-varying climatic response. *Clim Dyn* 44:791–806.
77. Tolwinski-Ward SE, Evans MN, Hughes MK, Anchukaitis KJ (2011) An efficient forward model of the climate controls on interannual variation in tree-ring width. *Clim Dyn* 36:2419–2439.
78. Tolwinski-Ward SE, Anchukaitis KJ, Evans MN (2013) Bayesian parameter estimation and interpretation for an intermediate model of tree-ring width. *Clim Past* 9: 1481–1493.
79. Huang J, van den Dool HM, Georgakakos KP (1996) Analysis of model-calculated soil moisture over the United States (1931–1993) and applications to long-range temperature forecasts. *J Clim* 9:1350–1362.
80. Evans MN, et al. (2006) A forward modeling approach to paleoclimatic interpretation of tree-ring data. *J Geophys Res* 111:G03008.
81. Touchan R, Shishov VV, Meko DM, Nouiri I, Grachev A (2012) Process based model sheds light on climate sensitivity of Mediterranean tree-ring width. *Biogeosciences* 9:965–972.
82. Mina M, Martin-Benito D, Bugmann H, Cailleret M (2016) Forward modeling of tree-ring width improves simulation of forest growth responses to drought. *Agric Meteorol* 221:13–33.
83. Linares JC, Camarero JJ, Carreira JA (2009) Plastic responses of *Abies pinsapo* xylogenesis to drought and competition. *Tree Physiol* 29:1525–1536.
84. Zuur AF, Ieno EN, Walker N, Saveliev AA, Smith GM (2009) *Mixed Effects Models and Extensions in Ecology with R* (Springer, New York).
85. Pinheiro J, Bates D, DebRoy S, Sarkar D (2009) *nlme*: Linear and Nonlinear Mixed Effects Models. R package Version 3.1-96. Available at cran.r-project.org/web/packages/nlme/index.html. Accessed April 15, 2017.
86. Sass-Klaassen U, et al. (2016) A tree-centered approach to assess impacts of extreme climatic events on forests. *Front Plant Sci* 7:1069.
87. Cavin L, Jump AS (2017) Highest drought sensitivity and lowest resistance to growth suppression are found in the range core of the tree *Fagus sylvatica* L. not the equatorial range edge. *Glob Change Biol* 23:362–379.